EFFECT OF THE FIRING TEMPERATURE ON THE PROPERTIES OF AL $_2$ O $_3$ /GLASS COMPOSITES

ANDREA SIMON1 – GÁBOR MUCSI2 – ISTVÁN KOCSERHA3

Abstract: Nowadays, ceramic materials having adequate strength and good electrical insulating properties, but also can be sintered at relatively low temperatures, play an increasingly important role. Ceramics providing this property combination are the glass-composite ceramics. The low-temperature sintering is ensured by the glass powder added to the base ceramic (which is usually alumina). Glass is typically a well-designed oxide frit that is sintered and melts/softens below 1,000 °C.

In this research work, the effect of firing temperature on the properties of glass/ceramic composite ceramics was studied. The samples were prepared by injection moulding technology. Density, porosity, flexural and compressive strength, thermal conductivity of the fired samples was measured. The morphology and the phases of the fired products were also analyzed.

Keywords: glass/ceramic composite, microstructure, injection moulding, sintering

INTRODUCTION

Glass-ceramic composites are increasingly being researched in the world of ceramics due to their well-controlled, individually adjustable properties [1–17]. In glass-ceramic composites, the main phase is a dielectric material having a high sintering temperature [8]. This crystalline phase provides the appropriate dielectric properties. The glass phase increases the dielectric loss but reduces the relative permittivity and the sintering temperature (depending on the composition of the glass) [8].

The shrinkage process of the composite is controlled by the viscous flow of the glass and the reactions taking place at the alumina/glass interface [1]. During sintering, the alumina dissolves in the glass and changes its composition. As a consequence, instead of cristoballite, other phases, e.g. anortite, albite are formed in the interfacial layer [1–3, 10, 13–14]. The formation of cristoballite limits the efficiency of the ceramic substrate when used on circuit boards [16]. An adequate amount (min. 10–20 V/V%) of Al₂O₃ and sintering at 900 °C at least is required to prevent the

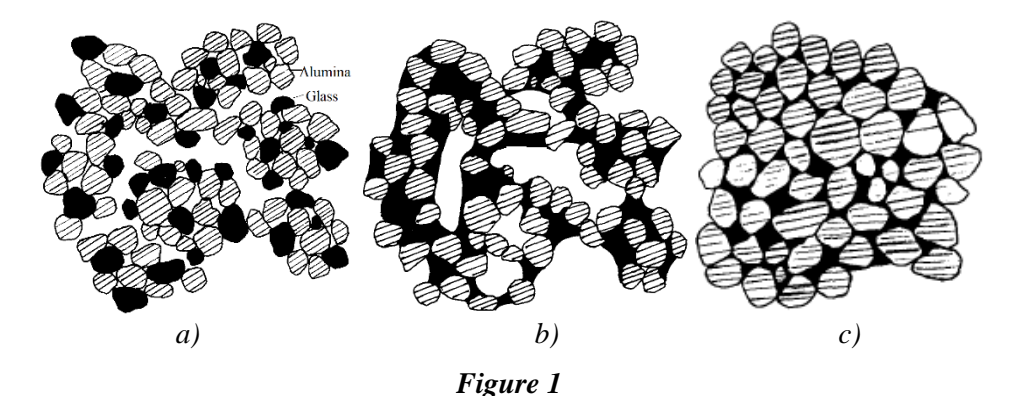
Institute of Ceramic and Polymer Engineering, University of Miskolc H-3515 Miskolc-Egyetemváros, Hungary simon.andrea@uni-miskolc.hu

Cerlux Ltd.
 H-5900 Orosháza, Csorvási 68., Hungary gabor.mucsi@cerlux.hu

Institute of Ceramic and Polymer Engineering, University of Miskolc H-3515 Miskolc-Egyetemváros, Hungary fempityu@uni-miskolc.hu

formation of cristoballite. The intensity of crystallization increases with temperature, however, firing at 1,100 °C increases the proportion of amorphous phase again [2–3]. When firing at a temperature of about 700 °C, partial dissolution of Al_2O_3 in the low viscosity glass phase begins and continues up to 800 °C. The anortite phase begins to crystallize from the glass phase at 875 °C on the surface of the Al_2O_3 particles. The weight fraction of anortite increases with the temperature until it stabilizes at 950 °C or higher [6]. The addition of Al_2O_3 prevents the formation of cristoballite, because during sintering Al_3 + ions diffuse into the glass and a strong bond can develop between Al_3^+/Al_2O_3 and the Na_3^+/K_3^+ ions of the glass, leading to changes in the structure and composition of the glass [7, 16–17].

Because the aluminum ion acts as a glass former, its dissolution in the glass reduces the amount of non-bridging oxygen ions, which significantly increases the viscosity of the glass. This phenomenon becomes more and more significant with the decrease in the particle size of alumina. It follows that the dissolution of alumina in glass slows the shrinkage of glass/alumina composites [1]. Shrinkage is also significantly influenced by the firing temperature, when examined between 900–1,100 °C, it initially increases with the sintering temperature, reaches a maximum value around 1,000 °C then decreases. During liquid-phase sintering, the viscosity of the glass melt decreases with increasing temperature, which in turn increases the densification due to rearrangement and changes in surface tension [4, 12]. Above 1,000 °C, the dissolution of alumina becomes more and more intense, as a result of which the viscosity of the glass melt increases, which slows down the grain rearrangement required for shrinkage [4, 18–20].



Schematic representation of the sintering process: a) green (pressed) glass/alumina composite, b) less densified structure (partly due to early neck solidification), c) well-densified structure [4]

Early solidification of the neck results in the formation of a solid alumina network that slows densification at higher temperatures, as this structure is difficult to break up due to the very high viscosity of the alumina-rich, liquid glass phase (*Figure 1*) [4, 20]. The glass/ceramic composite begins to densify at the temperature where the viscosity of the glass phase decreases sufficiently, i.e. where the glass melt is formed,

since above this temperature the viscous flow promotes further sintering [6, 21–23]. According to other studies, maximum shrinkage can be achieved by sintering between 800-900 °C, and the density of the fired composites decreases by increasing the temperature further [9]. According to Kumar et al. [14], the sintering temperature should be below 1,050 °C to reduce the excess solubility of Al_2O_3 in the glass.

In summary, several aspects must be taken into account when determining the appropriate firing temperature. Firstly, the firing temperature of a material designed for LTCC (low temperature cofired ceramic) application should be below 950 °C in order not to exceed the melting point of the built-in metal parts (e.g. silver – 961 °C). Secondly, at least 800 °C is required for the complete removal of the organic components [8]. This temperature range also limits the composition of the adequate glasses. Glasses with low softening point (e.g. borosilicate) cannot be used, or at least not on themselves, only in combination with an other glass having a high softening point.

The optimal composition for the glass-ceramic composites was set in preliminary experiments. In this research work, the optimal firing temperature, which fulfil the main requirements for the glass-ceramic composites, was investigated. First, the temperature should be below $1,000\,^{\circ}\text{C}$ to avoid the excess solubility of Al_2O_3 in the glass. On the other hand, it has to ensure the appropriate physical and mechanical properties. To this end, scanning electron microscopy (SEM), X-ray diffraction (XRD), porosity (Archimedes method), thermal conductivity, compressive and flexural strength tests were performed on the fired samples.

1. MATERIALS AND METHODS

1.1. Sample preparation

Alumina (Elektrokorund, IMERYS), glass frit (FERROX Frits), paraffin and oleic acid were used to prepare the glass/ceramic composites. The powder mixture consisted of a 3: 2 alumina and glass. The feedstock contained the base and the binding materials in 4: 1 ratio. The injection mass was pre-heated in a direct mixer to 80 °C. Samples with different shapes and geometrical dimensions corresponding to the required tests were produced on Cerlux Ltd.'s self-developed, low-pressure injection moulding equipment. The pressure and the temperature of the injection moulding was 6 bar and 70 °C, respectively. Dimensions of the green, injection moulded samples are listed in *Table 1*.

Table 1
Dimensions of the green samples

Test sample	Diameter,	Height, mm	Width, mm	Length, mm	
	mm				
Compressive strength	10	11			
Flexural strength		6	6	100	
Thermal conductivity	30	12			

Binder removal was accomplished at 650 °C in a 48-hour heat treatment cycle, in a natural gas furnace. The samples were fired at a maximum temperature of 850–900–950–1,000–1,050–1,100 °C in a Nabertherm HT 40/18 laboratory furnace, at a heating rate of 60 °C/hour.

1.2. Test methods

The particle size distribution of the alumina and glass frit was determined with a Horiba LA-950 laser granulometer. The phases of the raw materials and the fired specimens were identified by a Rigaku Miniflex II (Cu Kα, 2θ 3–90°) tabletop X-ray diffractometer, with a PDXL2 software to evaluate the results. The Rietveld complete profile fitting procedure was used to quantify the phases. The chemical composition and the surface morphology of the materials was measured using a ZEISS scanning electron microscope equipped with an EDAX detector. The specimens suitable for flexural and compressive strength tests were made in different geometries in an injection moulding tool. Columns were used for the former and cylindrical samples for the latter. Strength measurements were made with an Instron 5,560 universal tensile-pressing equipment. The porosity of the products was calculated from the water absorption test, in which the samples were boiled for 3 hours then soaked for 24 hours. All measurements requiring statistical evaluation were performed on at least 20 samples. Thermal conductivity tests were conducted on cylindrical samples with a polished surface and a diameter of 30 mm. C-Therm TCi thermal conductivity device operating on the principle of the Modified Transient Plane Source (MTPS) technique was used. Measurements were performed at room temperature.

2. RESULTS

2.1. Raw materials

Based on the X-ray examinations performed, the alumina consists mainly of corundum (Al_2O_3), with small amounts of diaoyudaoite ($NaAl_{11}O_{17}$) and hibonite ($CaAl_{12}O_{19}$), which are artificial minerals formed during corundum production. The frit is completely amorphous.

Table 2
Oxide composition and particle sizes of the raw materials

Oxide composition, wt%								
	Na_2O	MgO	Al_2O_3	SiO_2	ZrO_2	K_2O	CaO	ZnO
Alumina	0.8		98.78				0.42	
Frit	2.47	2.69	6.21	58.28	8.78	2.78	11.10	7.70
Particle size, µm								
	D90	D50	D10	Aver-	Me-			
				age	dian			
Alumina	43.9	17.67	7.89	22.65	17.67			
Frit	22.54	10.52	4.34	12.33	10.50			

Table 2 shows the oxide composition and particle size distribution of the raw materials. Figure 2 represents the initial morphology of the materials. Alumina and frit are characterized by polyhedral particle shapes, both in terms of coarse and finer fractions.

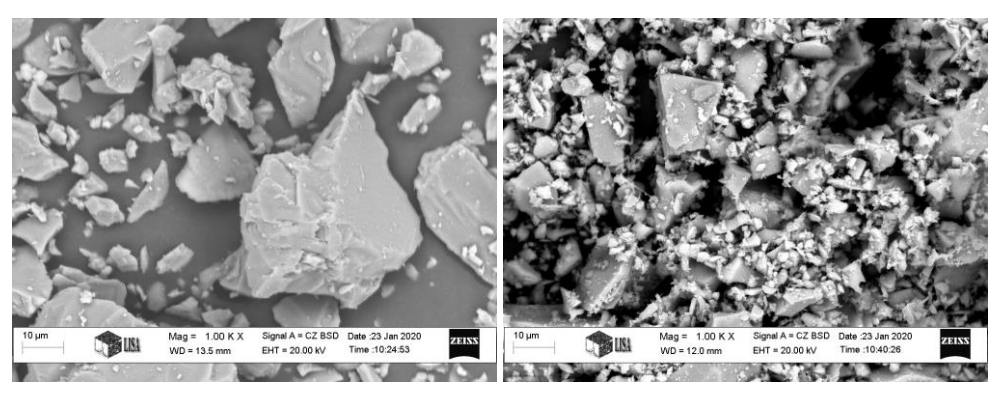
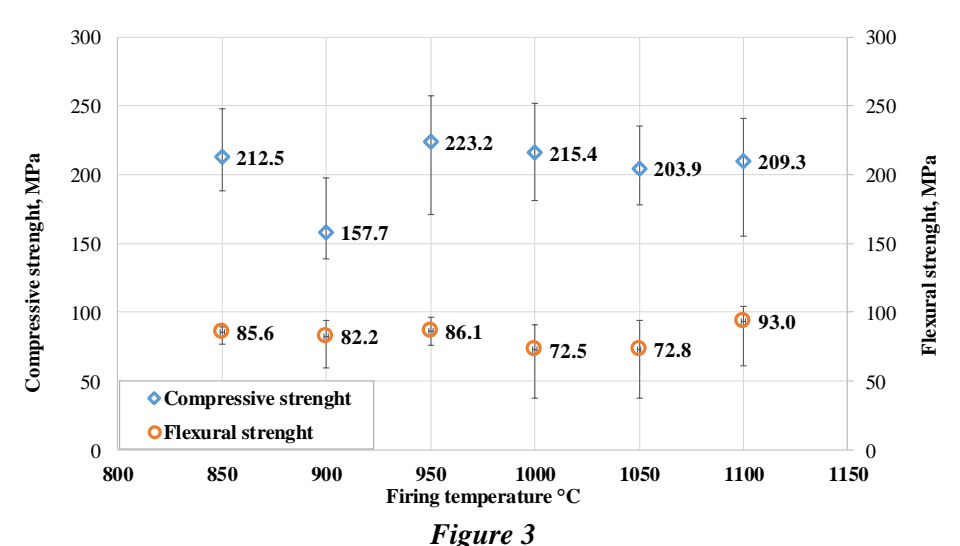


Figure 2 SEM micrographs of alumina and frit $(M = 1,000 \times)$

2.2. The effect of the firing temperature

Figure 3 shows the compressive and flexural strength of alumina/glass composites fired at 850–1,100 °C.



Compressive and flexural strength of the samples

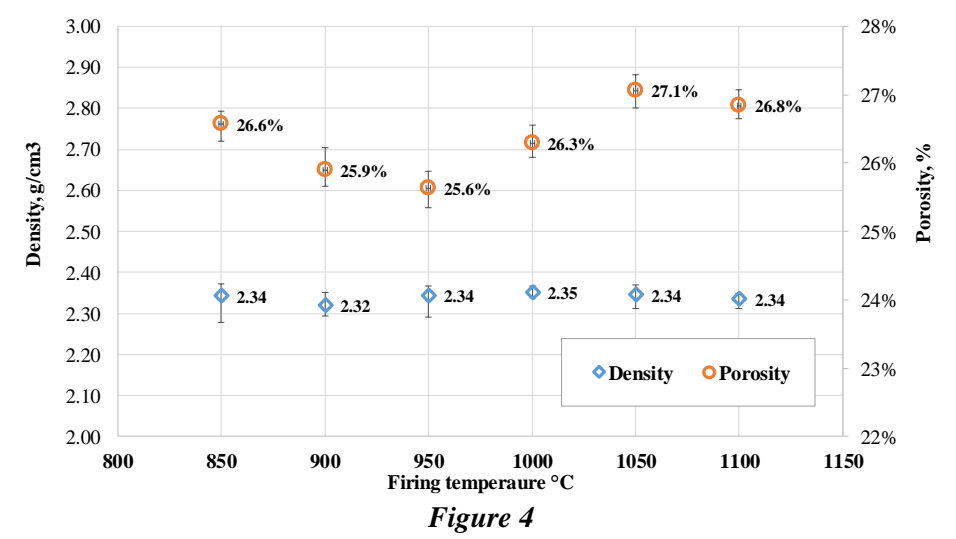
The effect of the firing temperature is not clear as the standard deviation of the results is quite large. The samples fired at 950 °C had the best combination of flexural and compressive strength. The compressive strength slightly reduces by increasing the firing temperature, but

the smallest temperature produced similar results. The samples fired at $900\,^{\circ}\text{C}$ presented the lowest strength.

Table 3
Average values of shrinkage, water absorption and thermal conductivity of the fired samples

	Firing temperature					
	850 °C	900 °C	950 °C	1000 °C	1050 °C	1100 °C
Shrinkage in diameter, %	3.98	3.92	3.84	4.06	4.00	3.94
Shrinkage in length, %	5.42	4.08	5.41	5.37	5.20	5.05
Average shrinkage, %	4.61	4.00	4.62	4.71	4.60	4.49
Water absorption, %	11.00	10.8	10.7	11.00	11.4	11.20
Thermal conductivity,	1.86	2.00	2.01	1.95	1.87	2.11
W/mK						

Figure 4 and Table 3 represents the results of the density, porosity and shrinkage, water absorption, thermal conductivity tests, respectively. The shrinkage in diameter did not change significantly, the difference between the sample sintered at 950 °C and 1,000 °C was only 5.5%. Along the height and length, samples sintered at 900 °C presented the lowest shrinkage. There is a similar trend in the values of water absorption and thermal conductivity. The density was not affected by temperature. The porosity value was the lowest at 950 °C, but it also differed only by 5.5% from the maximum value measured at 1,050 °C.

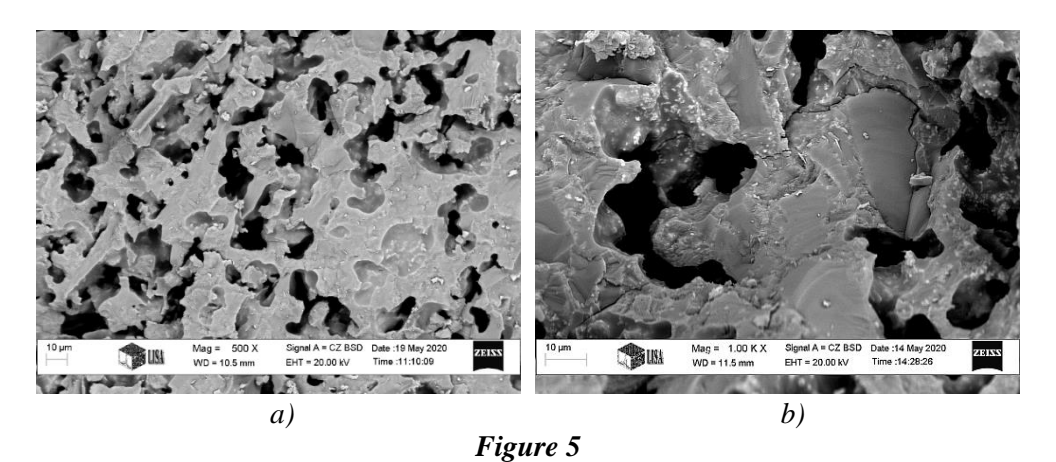


Density and porosity of the samples in the function of temperature

2.3. Morphology and phase analysis

Scanning electron micrographs of the fracture surface (*Figure 5*) show a pore system remained after the debinding. The pores, having a maximum size of a few 10 μm,

are inhomogeneously distributed. These micrographs underline the large variance in the strength data and the significant porosity values as well. Increasing the firing temperature did not change significantly the morphology of the fracture surfaces.



Microstructure of the alumina/glass composites sintered at 850 °C and 1,100 °C

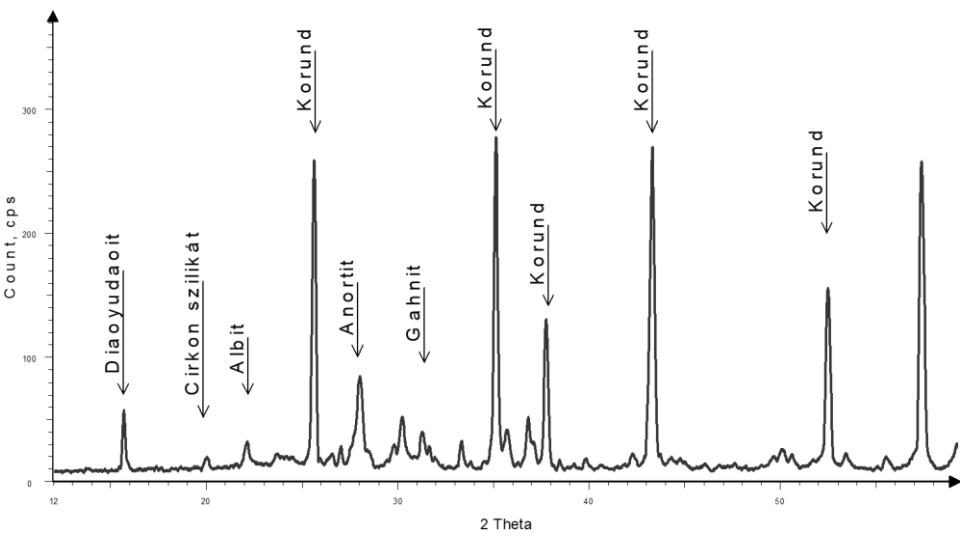


Figure 6
Phases of the samples fired at 850 °C

Based on the X-ray diffraction analysis, from the mixture of the starting crystalline corundum phase and the amorphous fritted glass phase, mainly crystalline phases are present in the sample fired at 850 °C, with an amorphous content of about 5%. The phases identified were corundum, albite, anortite, zirconium silicate, gahnite, and

diaoyudaoite (*Figure 6*). These phases remain up to 1,100 °C, but their amount varies slightly. In the sample sintered at 900 °C, the frit already started to melt, which increases the amount of amorphous phase to 22 wt%. It decreases to 16 wt% at 950 °C, indicating an increase in the proportion of the crystalline phase.

CONCLUSIONS

In this research, the effect of firing temperature on the properties of alumina/glass composites was studied. The melting behaviour of the frit and the debinding process affect mostly the main (non-electrical) properties of the samples. In the sintering range of 850–1,100 °C, the tested characteristics did not change significantly. The samples sintered at 900 °C had the lowest compressive strength and shrinkage. Based on the above measurements, the tested material can be fired even at 850 °C, since the higher firing temperatures do not provide significantly better properties.

ACKNOWLEDGMENTS

This research work is co-financed by the European Social Fund and the Government of Hungary within the framework of the project GINOP-2.1.2-8-1-4-16-2017-00219. The authors thank Árpád Kovács (Institute of Physical Metallurgy, Metal Forming and Nanotechnology) for the SEM micrographs and EDAX analyzes, dr. Tamás Mikó (Institute of Physical Metallurgy, Metal Forming and Nanotechnology) for his help in the compressive strength tests, Nora Papne Halyag (Faculty Of Earth Science And Engineering) for the laser granulometry tests, Károly Gál for the water absorption measurements, and Ildikó Tasnádi for the help in the flexural strength tests.

REFERENCES

- [1] Fang, Yu-Ching, Jean, Jau-Ho (2007). Effects of Alumina on Densification of a Low-Temperature Cofired Crystallizable Glass+Alumina System. *Japanese Journal of Applied Physics*, Vol. 46, No. 6A, pp. 3475–3480.
- [2] Jean, Jau-Ho, Fang, Yu-Ching, Dai, Steve X., Wilcox, David L. (2003). Effects of Alumina on Devitrification Kinetics and Mechanism of K₂O–CaO–SrO–BaO–B₂O₃–SiO₂ Glass. *Jpn. J. Appl. Phys.*, Vol. 42, Part 1, No. 7A, pp. 4438–4443., July 2003.
- [3] Dursun, Gülsüm Meryem, Duran, Cihangir (2019). Glass alumina composites for functional and structural applications. *Ceramics International*, 45, pp. 12550–12557.
- [4] Kumar, K. P., Ramesh, R., Seshan, K., Prasad, V. C. S. (1990). Liquid-phase sintering of lead borosilicate glass-alumina composite *Journal of Materials Science Letters*, 9, pp. 663–665.
- [5] Makarovič, Kostja, Meden, Anton, Hrovat, Marko, Holc, Janez, Benčan, Andreja, Dakskobler, Aleš, Belavič, Darko, Kosec, Marija. *The Effect of the*

- Firing Temperature on the Properties of LTCC. https://pdfs.semanticscholar.org/742a/ 32f8acadf54f52368387987f9f5f3584e38a.pdf, Accessed on 16/03/2020.
- [6] Suprapedi, Muljadi, Ramlan (2018). Effect of Addition of Amorphous Glass (Soda Lime Glass) on Sintering Process and Properties of Alumina Ceramics. *IOP Conf. Series: Journal of Physics: Conf. Series*, 1120, p. 012038.
- [7] Lima, M. M. R. A., Monteiro, R. C. C., Graça, M. P. F., Ferreira da Silva, M. G. (2012). Structural, electrical and thermal properties of borosilicate glass–alumina composites. *Journal of Alloys and Compounds*, 538, pp. 66–72.
- [8] Lima, M. M. R. A., Monteiro, R. C. C. (2006). Shrinkage Behaviour of Borosilicate Glass-Al₂O₃ Composites during Isothermal Sintering. *Materials Science Forum*, Vol. 514–516, pp. 648–652.
- [9] Li, Bo, Xu, Yang, Zhang, Shuren (2015). The Size-Effect of Al₂O₃ on the Sinterability, Microstructure and Properties of Glass-Alumina Composites. *Glass Physics and Chemistry*, Vol. 41, No. 5, pp. 503–508.
- [10] Margarida, M., Lima, R. A., Monteiro, C. C. (2008). Viscous Sintering in a Glass-Alumina System. *Materials Science Forum*, Vol. 587–588, pp. 143–147.
- [11] Higby, I., Shelby, James E. (1983). Properties of Glass/Alumina Composites. *Communications of the American Ceramic Society*, December 1983, C-229.
- [12] Zhu, Qingshan, de With, Gijsbertus, Dortmans, Leonardus J. M. G., Feenstra, Frits (2005). Near net-shape fabrication of alumina glass composites. *Journal of the European Ceramic Society*, 25, pp. 633–638.
- [13] Xia, Qin, Zhong, Chao-Wei, Luo, Jian (2014). Low temperature sintering and characteristics of K₂O–B₂O₃–SiO₂–Al₂O₃ glass/ceramic composites for LTCC applications. *J. Mater. Sci: Mater. Electron.*, 25, pp. 4187–4192.
- [14] Kumar, K. P., Prasad, V. C. S., Mukherjee, P. S., Mukunda, P. G. (1989). Behaviour of Lead Borosilicate Glass/Alumina Composite in the Temperature Range 900–1100 °C. *Materials Science and Engineering*, B5, pp. 1–4.
- [15] SebastianM. T., Jantunen, H. (2008). Low loss dielectric materials for LTCC applications: a review. *International Materials Reviews*, Vol. 53, No. 2, pp. 57–90.
- [16] El-Kheshen, A. A. (2003). Effect of alumina addition on properties of glass/ceramic composite. *British Ceramic Transactions*, Vol. 102, No. 5, pp. 205–209.
- [17] Jean, Jau-Ho, Chang, Chia-Ruey, Chang, Ruey-Ling, Kuan, Tong-Hua (1995). Effect of alumina particle size on prevention of crystal growth in low-k silica dielectric composite. *Materials Chemistry and Physics*, 40, pp. 50–55.

- [18] Monteiro, R. C. C., Lima, M. M. R. A. (2003). Effect of compaction on the sintering of borosilicate glass/alumina composites. *Journal of the European Ceramic Society*, 23, pp. 1813–1818.
- [19] Palanisamy, P., Sarma, D. H. R., West, R. W. (1985). Liquid-Phase Sintering in Thick-Film Resistor Processing. *J. Am. Ceram. Soc.*, 68, 1, C215–216.
- [20] Shiou, B. I., Hsu, W.-Y., Duh, J.-G. (1988). Fabrication and electrical behavior of liquid phase sintered zirconia. Ceramics International. *Ceram. Int.*, 14, p. 7.
- [21] Kemethmüller, S., Hagymasi, M., Stiegelschmitt, A., Roosen, A. (2007). Viscous Flow as the Driving Force for the Densification of Low-Temperature Co-Fired Ceramics. *Journal of the American Ceramic Society*, 90 (1), pp. 64–70.
- [22] Cole, S., Wellfair, G. (1974). High temperature viscosity control in multi-layer glasses a new concept. *Proceedings of the ISHM Symposium*, Boston, Massachusetts, pp. 25–34.
- [23] Simon, A., Lipusz, D., Györffy, B., Kristály, F., Gácsi, Z. (2013). Properties of Al2O3-glass composites. In: Meo, M. (ed.). 9th International Conference on composite science and technology, DEStech Publications, pp. 702–711.